Silicon on-chip bandpass filters for the multiplexing of high sensitivity photonic crystal microcavity biosensors

Hai Yan, Yi Zou, Swapnajit Chakravarty, Chun-Ju Yang, Zheng Wang, Naimei Tang, Donglei Fan, and Ray T. Chen

Articles you may be interested in

Analysis of ultra-high sensitivity configuration in chip-integrated photonic crystal microcavity bio-sensors
Appl. Phys. Lett. **104**, 191109 (2014); 10.1063/1.4875903

On-chip microfluidic biosensor using superparamagnetic microparticles
Biomicrofluidics **7**, 054117 (2013); 10.1063/1.4826546

Gold nanoring as a sensitive plasmonic biosensor for on-chip DNA detection
Appl. Phys. Lett. **100**, 173114 (2012); 10.1063/1.4707382

On-chip single photon emission from an integrated semiconductor quantum dot into a photonic crystal waveguide
Appl. Phys. Lett. **99**, 261108 (2011); 10.1063/1.3672214

On-chip silicon-based active photonic molecules by complete photonic bandgap light confinement
Appl. Phys. Lett. **99**, 034105 (2011); 10.1063/1.3614548

Silicon on-chip bandpass filters for the multiplexing of high sensitivity photonic crystal microcavity biosensors

Hai Yan,[1,a)] Yi Zou,[1] Swapnajit Chakravarty,[2,b)] Chun-Ju Yang,[1] Zheng Wang,[1,3] Naimei Tang,[1,2] Donglei Fan,[3,4] and Ray T. Chen[1,2,c)]

[1]*Department of Electrical and Computer Engineering, Microelectronics Research Center, The University of Texas at Austin, 10100 Burnet Rd., Austin, Texas 78758, USA*
[2]*Omega Optics, Inc., 8500 Shoal Creek Blvd., Austin, Texas 78757, USA*
[3]*Materials Science and Engineering Program, Texas Materials Institute, The University of Texas at Austin, Austin, Texas 78712, USA*
[4]*Department of Mechanical Engineering, The University of Texas at Austin, Austin, Texas 78712, USA*

A method for the dense integration of high sensitivity photonic crystal (PC) waveguide based biosensors is proposed and experimentally demonstrated on a silicon platform. By connecting an additional PC waveguide filter to a PC microcavity sensor in series, a transmission passband is created, containing the resonances of the PC microcavity for sensing purpose. With proper engineering of the passband, multiple high sensitivity PC microcavity sensors can be integrated into microarrays and be interrogated simultaneously between a single input and a single output port. The concept was demonstrated with a 2-channel L55 PC biosensor array containing PC waveguide filters. The experiment showed that the sensors on both channels can be monitored simultaneously from a single output spectrum. Less than 3 dB extra loss for the additional PC waveguide filter is observed. © 2015 AIP Publishing LLC. [http://dx.doi.org/10.1063/1.4916340]

Photonic crystal (PC) microcavities side-coupled to photonic crystal waveguides (PCWs) have been demonstrated as a competitive candidate for high-sensitivity biosensors.[1–8] The ability of PC microcavities to confine light to ultra-small mode volumes promises the potential for high-density microarrays with slow light enhanced sensitivity to refractive index changes of the ambient. Biosensor microarrays have been demonstrated with multiplexed PC microcavities for the specific detection of lung cancer cell line lysates,[3] allowing the specific detection of different biomolecules on the same chip.

Biomedical diagnostics require both specific binding reactions and control test to be performed and monitored preferably at the same time on the same chip. For the above-mentioned biosensor microarrays,[3] multiple optical fibers or a fiber array at the output is necessary in order to monitor the binding reactions from all PC microcavities simultaneously. However, from the application perspective, when designing a portable device, with limited space for off-chip optical components, one needs to maximize the number of sensors that can be simultaneously interrogated with a single input and output, making the packaging and alignment robust and cost-effective.

Towards this direction, we have investigated the series connection of L3 PC cavity sensors (formed by three missing holes and has a single resonance in the transmission spectrum). We demonstrated that five L3 PC microcavities can be connected in series between a single input port and a single output port.[9] However, the sensitivity of L3 PC sensors are relatively low in comparison with longer PC microcavities such as the L13, L21, and L55 PC microcavities

(formed by 13, 21, and 55 missing holes, respectively).[5,10] Longer PC microcavities provide higher quality factor and more surface area for light-matter interaction, resulting in higher sensitivity and lower detection limit, which is pivotal for low-concentration biomarker detection like the early cancer diagnosis. The L55 PC biosensors were reported to have a minimum detection limit of 50 femto-molar.[10] However, longer PC microcavities have several resonances in the transmission spectrum which makes them difficult to multiplex.

In this paper, we propose a scheme to multiplex multi-resonance PC cavity sensors between a single input and output. An additional PCW bandpass filter is integrated on each channel of a multiplexed sensor array to select a narrow wavelength band that filters a specific resonance or resonances of a long PC microcavity. All channels are then connected in parallel, enabling all sensors to be interrogated simultaneously between a single input optical fiber and a single output optical fiber.

Other on-chip photonic bandpass filters based on silicon-on-insulator (SOI) substrates, such as waveguide Bragg gratings, microring resonators, and arrayed waveguide gratings (AWGs), were also considered against the PCW filter used in this paper. However, the footprint of AWGs are usually too large (for example, 200 by 350 μm^2 in Ref. [11]), which are not suitable for dense integration. Waveguide Bragg gratings are usually quite long (over 0.5 mm) and need to work in reflection mode,[12–14] while for microring resonators, high-order coupled ring structures[15–17] are necessary to achieve a wide and sharp passband (5–10 nm) for the application here. Both are highly sensitive to fabrication variations. PCW filter is a natural choice since the biosensor is also made from PC, which makes the passband alignment easier.

A line defect in a 2D photonic crystal lattice on a thin slab forms a PCW, whose typical transmission spectrum is

---

a)Electronic mail: hai.yan@utexas.edu
b)Electronic mail: swapnajit.chakravarty@omegaoptics.com.
c)Electronic mail: raychen@uts.cc.utexas.edu
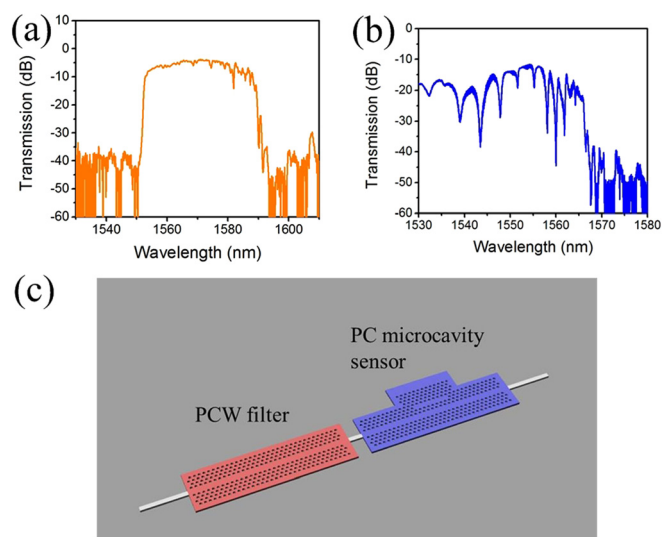
106, 121103-1

FIG. 1. Transmission spectra of (a) a PCW and (b) a PC microcavity sensor. (c) Proposed PCW bandpass filter for PC sensor, formed by series-connected PCW and PC microcavity sensor.

shown in Fig. 1(a). A passband is observed in the transmission spectrum. Light with longer wavelength above the passband lies in the band gap of the photonic crystal and is not guided. Shorter wavelengths outside the passband are above the light line of the cladding material and thus cannot be well-confined in the waveguide. When a PC microcavity is side-coupled to the PCW, resonances appear in the transmission spectrum (Fig. 1(b)). The resonance filter is created by connecting the above two PC regions in series (Fig. 1(c)). The lattice constants of both the PC regions can be engineered so that a narrower passband is formed in the transmission spectrum, where the rising edge comes from the light line of the first PCW (acts as a filter) and the falling edge from the guided mode transmission band edge of the second PCW (the one with PC microcavity). The PCW filter filters out the resonances of the PC microcavity outside the passband without altering the spectrum of the PC microcavity within the passband. The resonances within the passband can be used for sensing when analyte solutions flow on the PC cavity surface. SU-8 layer on the PCW filter serves as a protection layer from sensing fluids and is open on top of the PC microcavity.

With proper engineering of the passband width and position, several high sensitivity multi-resonance L55 PC microcavity sensors can be multiplexed into a single-input and single-output system by employing the proposed structure as

portrayed in Fig. 2(a). Two PC sections are employed for each channel. The first one functions as a wavelength filter and the second as the biosensing site with a cascaded transmission band in reference to the adjacent channels. Fig. 2(b) shows the corresponding spectrum for each channel. The passbands are carefully designed to avoid any overlap with each other. Multiple sensors now can be interrogated simultaneously from the transmission spectrum of the single output port. These sensors allow different receptor biomolecules to be immobilized on each of them using ink-jet printing technique,[5] so that different biomarkers within a bio-sample can be studied. Alternatively, the sensors can also be connected in separate microfluidic channels to enable the test of different samples at the same time.

For proof-of-concept demonstration of the proposed PCW filter and multiplexing, a 2-channel PC biosensor array was designed and fabricated (Fig. 3). 1×2 multimode interference (MMI) coupler and Y-junction were used to split and combine the waveguides. A W1 PCW side-coupled with L55 PC microcavity is fabricated on one arm. On the second arm, a W1 PCW is side-coupled with L55 microcavity biosensor and then connected in series with a W1 PCW filter. The lattice constant of the L55 PC microcavity in the second arm is smaller than that of the L55 PC microcavity in the first arm. Hexagonal structure with a uniform lattice constants of 388 nm, 396 nm, and 390 nm are adopted, respectively, for L55 PC cavity on the first arm, for L55 PC cavity on the second arm, and the PCW filter. The silicon slab thickness is 250 nm, while the air hole diameters for PC microcavity and PCW filter are 216 nm and 170 nm, respectively. Group index tapers in each PCW efficiently couple light into the slow light region from a regular channel waveguide.[18] Subwavelength grating couplers were used as the interface between waveguides and optical fibers.[19]

The devices were patterned by e-beam lithography on a silicon-on-insulator wafer, followed by reactive ion etching to transfer the pattern onto the silicon layer. SU-8 polymer was subsequently coated on the chip surface. The SU-8 above the sensor region was removed through photolithography to open a window for sensing purpose. SU-8 remained on top of the PCW filter.

Transmission spectra of the fabricated devices were obtained from a testing platform using a broadband amplified spontaneous emission (ASE) source (1510 nm–1630 nm) and an optical spectrum analyzer (OSA). Light from the ASE source was guided through a polarizer to the grating coupler on the chip and excites fundamental transverse electric (TE)
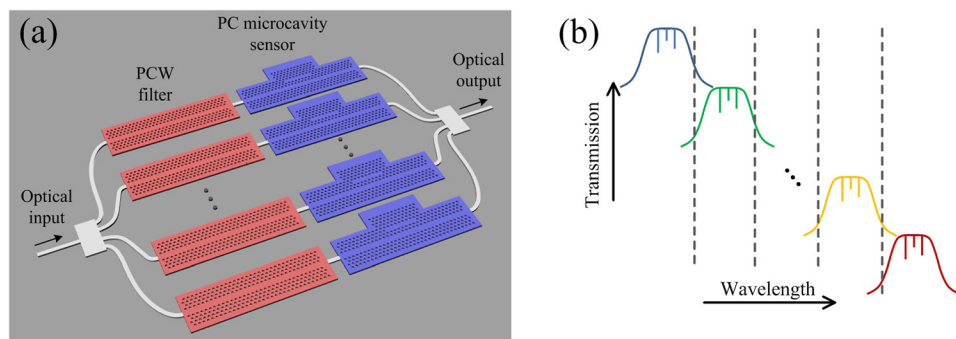

FIG. 2. (a) Proposed single-input single-output PC biosensor array and (b) the corresponding transmission spectra from each channel. Resonances from the coupled PC cavity still exist within the passband.
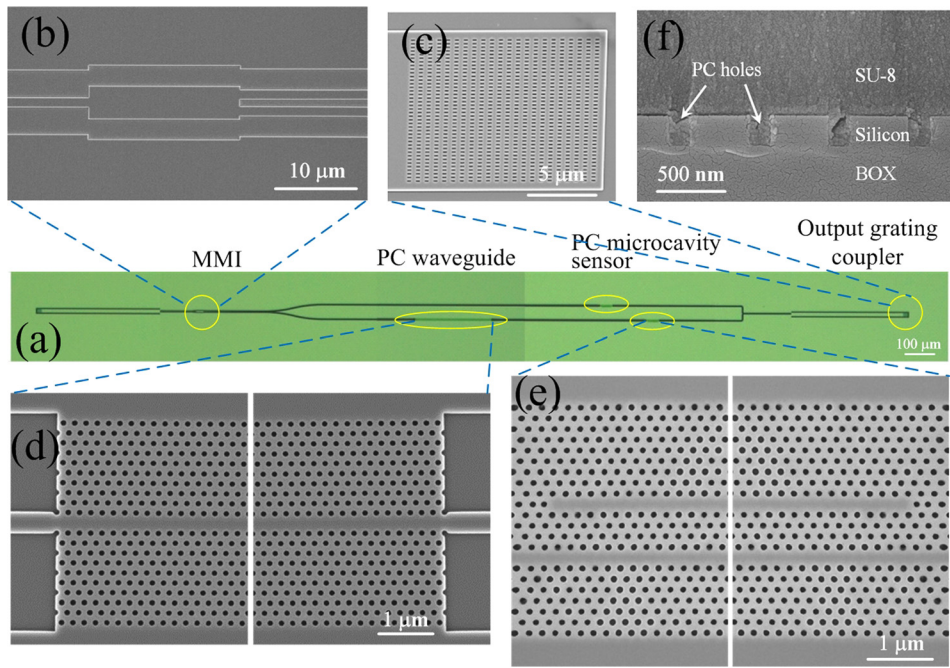
FIG. 3. (a) Microscopic image of the fabricated 2-channel PC biosensor array (prior to SU-8 coating). On the upper channel, a single PC microcavity biosensor with a = 388 nm is located. On the lower channel, PCW filter is connected in series with the PC microcavity biosensor with a = 396 nm. Input and output grating couplers are indicated. SEM images of (b) MMI coupler, (c) subwavelength grating, (d) the PCW filter, and (e) one of the PC microcavity sensors. (d) and (e) omit the central part of the devices and show the two ends of the devices. (f) SEM image of the cross section of the PCW filter coated with SU-8. The PC holes were completely filled by SU-8.

mode in the waveguides. Output light signal was collected by another fiber, and optical spectrum was generated by the OSA. During the test, the PC microcavity is measured with water ambient as a simulation of real biosensing application.

Fig. 4(a) shows the measured transmission spectrum for the fabricated device shown in Fig. 3(a). The thickness of the SU-8 is 0.42 μm. From the spectrum, we can clearly see the resonances for the L55 PC cavities on both channels. Resonances in the region of 1525–1550 nm are from the L55 on the upper channel (with designed lattice constant of 388 nm), while the resonances within the range of 1560–1580 nm are from the other L55 on the lower channel (with designed lattice constant of 396 nm). This 20 nm passband range for the lower channel is formed by the cutting edge (~1560 nm) of the PCW filter and the band-edge (~1580 nm) of the PCW (to which L55 cavity is coupled). Without the PCW filter, the resonances with wavelengths shorter than 1560 nm would overlap with the resonances from the other L55 cavity in the first channel, because the transmission passband for this PC cavity can be as wide as over 40 nm (see Fig. 1(b)). In Fig. 4(a), we can also see that the additional loss from the PCW filter is about 3 dB by

comparing the transmission for both channels. Same PC device but with uncombined output ports were also fabricated and measured on the same chip. The spectrum is shown in Fig. 4(b), where black and red curves represent the two channels measured separately, which verifies the above analysis in combined device.

The sensors were characterized in a bulk refractive index sensing test, in which the PC sensor in channel 2 was covered with SU-8 ($n = 1.575$), while the PC sensor in channel 1 was still measured in water ($n = 1.318$). The obtained spectrum is shown in Fig. 4(c) against the original spectrum measured in water. As expected, there is no resonance shift for channel 1 while about 16 nm red shift for channel 2 (corresponds to a sensitivity of 62 nm/RIU). The test demonstrates that sensors from different channels can work separately with their resonance shift being monitored in a single transmission spectrum. It is worth noting that in PC based biosensing applications, the resonance shifts are typically within 2 nm (Refs. 3, 5, 7 and 10) and the spectrum will not change as dramatically as shown in Fig. 4(c).

In order to obtain a sharp edge in the passband, which will provide a better signal to noise ratio, we tested PCW
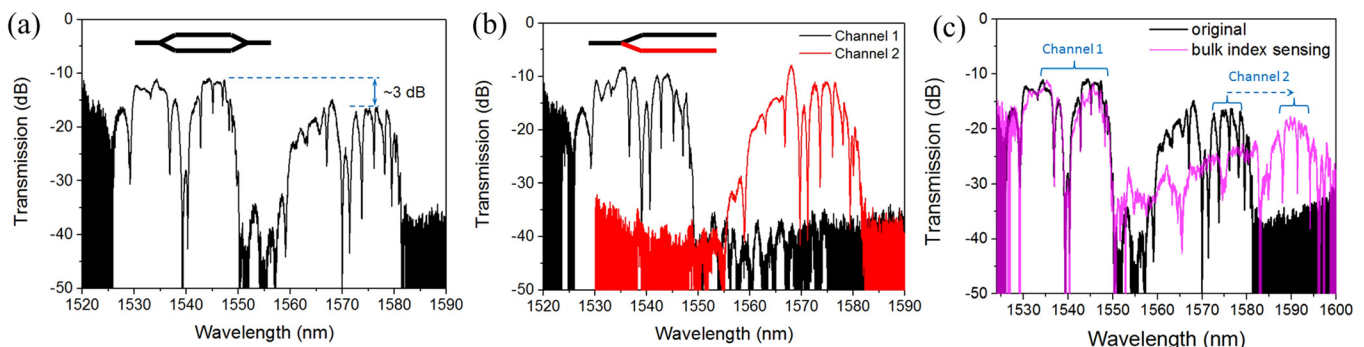

FIG. 4. Measured transmission spectra from (a) the device in Fig. 3(a) with a single output port and (b) a same device but with separated output ports, as schematically represented in the insets. SU-8 cladding has a thickness of 0.42 μm. (c) Bulk refractive index sensing spectrum versus original spectrum: the PC sensor in channel 2 is covered with SU-8 and thus shows resonance shift while the sensor in channel 1 is not affected.

filters with various lengths (number of periods) and with different thicknesses of top claddings (SU-8). The design for the PCW filter in Fig. 3(a) is a 250 μm long PCW with 16 periods of input and output group index tapers[18] at a = 390 nm. The total number of periods is 672. Fig. 5(b) shows the transmission spectra of PCW filters with four different lengths, starting with 72 periods in steps of 200 periods. The PCW filter is coated with 0.42 μm thick SU-8. In the transmission spectra, the rising edge becomes increasingly sharper with increasing length of the PCW. The roll-off increases from 0.33 dB/nm for 72 periods to 4 dB/nm for 672 periods. This roll-off increase of the rising edge arises from the light line of the cladding layer. Above the light line, i.e., with shorter wavelength, the waveguide mode is less confined in the vertical direction through total internal reflection, which causes additional loss. The loss is more significant for longer PCWs as the light path becomes longer.[20] The light line position can be located easily from the dramatic rise in the transmission intensity of the 672-period PCW (black curve in Fig. 5(b)).

On the other hand, the thickness of the SU-8 cladding layer affects the effective refractive index of the top cladding and thus the effective position of the light line of the top cladding. Fig. 5(a) shows the dispersion diagram of the W1 PCW on silicon substrate with SU-8 top cladding simulated with 3D plane wave expansion method. There are two light lines corresponding to top and bottom claddings, i.e., SU-8 ($n = 1.575$) and silicon dioxide ($n = 1.460$), respectively. λ_1 represents the band edge of the PCW, which is approximately at the position where n_g is 35 in the fabricated device.[21] λ_2 is the critical wavelength at which the optical mode is still well confined within top and bottom claddings. λ_3 is the critical wavelength at which the mode no longer is totally reflected at the boundary between silicon and buried oxide layer. With thick SU-8 top cladding, the passband in the transmission spectra (black curve in Fig. 5(c)) is between λ_1 and λ_2. However, if SU-8 is as thin as 0.42 μm, the evanescent tail of the propagation mode extends outside the SU-8 layer. As a result, the effective refractive index of the top cladding becomes smaller and the top cladding light line effectively shifts towards the silicon dioxide light line making the passband $\sim$10 nm wider, between λ_1 and λ_3 (blue curve of Fig. 5(c)). The 10 nm side band shown in the

transmission spectrum with 2 μm SU-8 (red curve of Fig. 5(c), between λ_2 and λ_3) clearly reflects the light line of both the silicon dioxide and the SU-8 claddings. The PCW filter in Fig. 4 (672 periods long with 0.42 μm SU-8) can further be optimized to obtain narrower bandwidth, shorter PCW length while keeping a sharp cutting edge by using thicker SU-8 cladding.

In this paper, instead of focusing on building the smallest sensor to increase the integration density of a sensor array, we also consider the size reduction in the system level (optical fibers, detectors) benefited from a single input and output sensor chip as well as the higher sensitivity provided by larger effective sensing area. From the above analysis, a 472-period PCW (around 175 μm in length, black curve in Fig. 5(c)) is enough to provide a usable filter response. This size still allows high density integration since the density is primarily limited by the smallest pitch of the receptor biomolecules solution that can be dispensed on the chip.

By optimizing parameters of the PCW filters, the passband can be as narrow as 5 nm to include at least one resonance and to allow resonance shift during biosensing test, thus, enabling the multiplexing of up to 16 sensing channels within the wavelength range of C band and L band. Also, we expect that our PC filters and sensors are relatively robust to fabrication variations because all PC air holes would be affected in similar ways. It will result in similar shifts in the transmission spectra of all PC components, which relaxes the fabrication requirement.

The PCW bandpass filter proposed here can also serve as an optofluidic spectral filter.[22,23] The passband can be pre-engineered easily by PC design and also highly reconfigurable when integrated with microfluidics, which allows both localized control and high refractive index modulation.[24] This type of optofluidic filter is a promising component in future lab-on-chip systems.

In summary, a method to multiplex high sensitivity multi-resonance L55 PC microcavity biosensors for simultaneous measurement between a single fiber input and single fiber output was proposed and demonstrated. PCW filters were used to filter a narrow band containing resonances of the PC biosensors so that the PC biosensors can be connected in parallel without resonance overlap. The concept was demonstrated through a 2-channel L55 PC biosensor array and
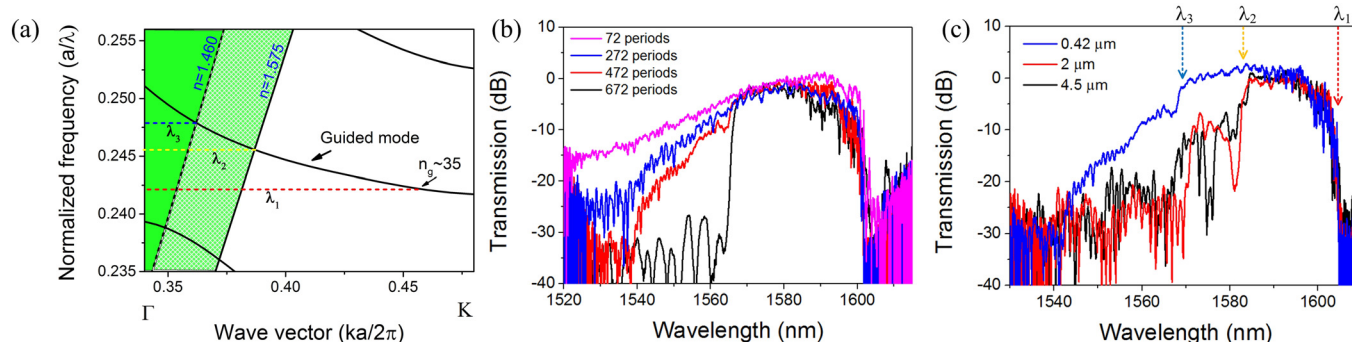
FIG. 5. (a) Simulated dispersion diagram of W1 PCW on SOI substrate with SU-8 polymer as top cladding. The two light lines correspond to the top cladding ($n = 1.575$) and buried oxide ($n = 1.460$), respectively; (b) Transmission spectra of W1 PCWs with different lengths; (c) Transmission spectra of W1 PCW (472 periods long) with three different thicknesses of SU-8 top claddings. λ_1, λ_2, and λ_3 correspond to those in the dispersion diagram in (a). Three different thicknesses of SU-8 were obtained by using MicroChem SU-8 2000.5, SU-8 2002, and SU-8 2005 with recommended spin program.

the sensing experiment showed that the two sensors can be monitored through a single output spectrum. Less than 3 dB extra loss is observed for the additional PCW filter.

[1]S. Pal, A. R. Yadav, M. A. Lifson, J. E. Baker, P. M. Fauchet, and B. L. Miller, Biosens. Bioelectron. **44**(0), 229–234 (2013).

[2]F. Liang, N. Clarke, P. Patel, M. Loncar, and Q. Quan, Opt Express **21**(26), 32306–32312 (2013).

[3]S. Chakravarty, W.-C. Lai, Y. Zou, H. A. Drabkin, R. M. Gemmill, G. R. Simon, S. H. Chin, and R. T. Chen, Biosens. Bioelectron. **43**, 50–55 (2013).

[4]Y. Zou, S. Chakravarty, W.-C. Lai, C.-Y. Lin, and R. T. Chen, Lab Chip **12**(13), 2309–2312 (2012).

[5]W. C. Lai, S. Chakravarty, Y. Zou, and R. T. Chen, Opt. Lett. **37**(7), 1208–1210 (2012).

[6]C. Kang, S. M. Weiss, Y. A. Vlasov, and S. Assefa, Opt. Lett. **37**(14), 2850–2852 (2012).

[7]S. Chakravarty, Y. Zou, W.-C. Lai, and R. T. Chen, Biosens. Bioelectron. **38**(1), 170–176 (2012).

[8]M. G. Scullion, A. Di Falco, and T. F. Krauss, Biosens. Bioelectron. **27**(1), 101–105 (2011).

[9]Y. Zou, S. Chakravarty, L. Zhu, and R. T. Chen, Appl. Phys. Lett. **104**(14), 141103 (2014).

[10]Y. Zou, S. Chakravarty, D. N. Kwong, L. Wei-Cheng, X. Xiaochuan, L. Xiaohui, A. Hosseini, and R. T. Chen, IEEE J. Sel. Top. Quantum Electron. **20**(4), 171–180 (2014).

[11]W. Bogaerts, S. K. Selvaraja, P. Dumon, J. Brouckaert, K. De Vos, D. Van Thourhout, and R. Baets, IEEE J. Sel. Top. Quantum Electron. **16**(1), 33–44 (2010).

[12]I. Giuntoni, A. Gajda, M. Krause, R. Steingruber, J. Bruns, and K. Petermann, Opt. Express **17**(21), 18518–18524 (2009).

[13]S. Zamek, D. T. H. Tan, M. Khajavikhan, M. Ayache, M. P. Nezhad, and Y. Fainman, Opt. Lett. **35**(20), 3477–3479 (2010).

[14]X. Wang, W. Shi, H. Yun, S. Grist, N. A. F. Jaeger, and L. Chrostowski, Opt. Express **20**(14), 15547–15558 (2012).

[15]B. E. Little, S. T. Chu, H. A. Haus, J. Foresi, and J. P. Laine, J. Lightwave Technol. **15**(6), 998–1005 (1997).

[16]J. V. Hryniewicz, P. P. Absil, B. E. Little, R. A. Wilson, and P. T. Ho, IEEE Photonics Technol. Lett. **12**(3), 320–322 (2000).

[17]F. N. Xia, M. Rooks, L. Sekaric, and Y. Vlasov, Opt. Express **15**(19), 11934–11941 (2007).

[18]C.-Y. Lin, X. Wang, S. Chakravarty, B. S. Lee, W.-C. Lai, and R. T. Chen, Appl. Phys. Lett. **97**(18), 183302 (2010).

[19]X. Xu, H. Subbaraman, J. Covey, D. Kwong, A. Hosseini, and R. T. Chen, Appl. Phys. Lett. **101**(3), 031109 (2012).

[20]L. O'Faolain, X. Yuan, D. McIntyre, S. Thomas, H. Chong, R. M. De La Rue, and T. F. Krauss, Electron. Lett. **42**(25), 1454–1455 (2006).

[21]X. Wang, C.-Y. Lin, S. Chakravarty, J. Luo, A. K. Y. Jen, and R. T. Chen, Opt. Lett. **36**(6), 882–884 (2011).

[22]P. Measor, B. S. Phillips, A. Chen, A. R. Hawkins, and H. Schmidt, Lab Chip **11**(5), 899–904 (2011).

[23]H. Schmidt and A. R. Hawkins, Nat. Photonics **5**(10), 598–604 (2011).

[24]D. Erickson, T. Rockwood, T. Emery, A. Scherer, and D. Psaltis, Opt. Lett. **31**(1), 59–61 (2006).